High Ferroelectricities and High Curie Temperature of $BiInO_3PbTiO_3$ Thin Films Deposited by RF Magnetron Sputtering Method *

Ke-xue Sun(孙科学)[1,2**], Shu-yi Zhang(张淑仪)[2], Kiyotaka Wasa[2,3]

[1]*College of Electronic and Optical Engineering, Nanjing University of Posts and Telecommunications, Nanjing 210023*
[2]*Key Laboratory of Modern Acoustics, Institute of Acoustics, Nanjing University, Nanjing 210093*
[3]*Faculty of Science, Yokohama City University, Yokohama 236-0027, Japan*

(Received 12 July 2018)

Properties of ferroelectric $xBiInO_3$-$(1-x)PbTiO_3$ (xBI-$(1-x)PT$) thin films deposited on (101) $SrRuO_3$/(200) Pt/(200) MgO substrates by rf magnetron sputtering method and effects of deposition conditions are investigated. The structures of the xBI-$(1-x)PT$ films are characterized by x-ray diffraction and scanning electron microscopy. The results indicate that the thin films are grown with mainly (001) orientation. The chemical compositions of the films are analyzed by scanning electron probe and the results indicate that the loss phenomena of Pb and Bi elements depend on the pressure and temperature during the sputtering process. The sputtering parameters including target composition, substrate temperature, and gas pressure are adjusted to obtain optimum sputtering conditions. To decrease leakage currents, 2 mol% La_2O_3 is doped in the targets. The P–E hysteresis loops show that the optimized xBI-$(1-x)PT$ ($x = 0.24$) film has high ferroelectricities with remnant polarization $2P_r = 80\,\mu C/cm^2$ and coercive electric field $2E_c = 300\,kV/cm$. The Curie temperature is about 640°C. The results show that the films have optimum performance and will have wide applications.

PACS: 43.90.+v, 43.35.+d, 68.60.Bs DOI: 10.1088/0256-307X/35/12/124301

To fabricate high performance ferroelectric devices, the ferroelectric materials should have large remnant polarization (P_r), coercive field (E_c) and high Curie temperature (T_c). Recently, great attention has been paid to studying ferroelectric materials with perovskite structures, such as lead zirconate titanate (PZT) based ferroelectric materials, because of high ferroelectricity and good temperature stability.[1–4] Generally, the Curie temperature (T_c) of PZT ferroelectric materials is around 386℃, and the effective operating temperature should be below half the Curie temperature, thus PZT devices are difficult to be applied to operate in an environment above 200℃. However, the ferroelectric devices may sometimes operate at high temperature for applications in automobile and aerospace industries. Therefore, it is important to develop ferroelectric materials with optimized electric properties and high T_c.[5]

Recently, perovskite-type $Bi(Me)O_3$-$PbTiO_3$ (Me: Sc, In, Y, Yb, etc.) solid solution systems as high-temperature ferroelectric ceramics have become popular research topics.[6,7] To obtain the miniaturization and high performance of electronic devices, researchers have focus on developing new thin film materials.[8–10] For example, Ko *et al.*[9] reported that 0.15BI-0.85PT ferroelectric polycrystalline thin films were grown on $PbTiO_3$-layer buffered silicon substrates by chemical solution deposition and showed that P_r and T_c could be $22\,\mu C/cm^2$ and 550℃, respectively. Meanwhile, Lee *et al.*[11] reported that 0.5 mol% Mn-doped epitaxial 0.15BI-0.85PT ferroelectric thin films grown on $PbTiO_3$ buffered substrates were prepared by pulsed laser deposition and showed that P_r and T_c could be $29\,\mu C/cm^2$ and 565℃, respectively. Lee *et al.*[12] also reported that 0.5 mol% Mn-doped epitaxial 0.20BI-0.80PT ferroelectric thin films have P_r and T_c to be $33\,\mu C/cm^2$ and 584℃, respectively. However, the ferroelectric properties of these films are not beyond those of PZT. Therefore, to explore $xBi(Me)O_3$-$(1-x)PbTiO_3$ thin films with high ferroelectric performance and high T_c has become an essential topic for fabricating high-temperature ferroelectric devices.

In this work, xBI-$(1-x)$PT thin films with mainly (001) orientated structure are deposited on MgO (200) substrates using the rf-magnetron sputtering method. The deposition conditions are adjusted carefully and the structures, ferroelectric and dielectric properties and Curie temperatures of the optimized thin films are investigated in detail.

An rf magnetron sputtering system is used to deposit thin films, in which powder targets are used.[13–15] The powder is packed into copper target tray with 7.5 cm in diameter. The xBI-$(1-x)$PT thin films are grown on (200) MgO substrates with (101) $SrRuO_3$ (SRO) buffer layers and (200) Pt bottom electrodes. The SRO films show excellent chemical and thermal stability, and enhance growth of mainly (001)

*Supported by the National Natural Science Foundation of China under Grant No 11304160, the Special Fund for Public Interest of China under Grant No 201510068, and the NUPTFC under Grant No NY215111.
**Corresponding author. Email: sunkx@njupt.edu.cn
© 2018 Chinese Physical Society and IOP Publishing Ltd

orientation of the xBI-$(1-x)$PT thin films. The mixed powders are composed of xBI-$(1-x)$PT, (x is adjusted between 0.2 and 0.3), near the morphotropic phase boundary (MPB) compositions, with additional PbO and Bi_2O_3 for compensating Pb and Bi evaporation losses at high temperature sputtering,[16,17] and doping La_2O_3 for decreasing leakage current occurrence of the thin films.[18] The sputtering gases are argon (Ar) and oxygen (O_2) mixture with the ratio of 20:1, and the total sputtering gas pressure is changed from 0.5 Pa to 2 Pa. The sputtering power is set at 64 W, and the substrates are maintained at 600℃–700℃. The sputtering conditions are listed in Table 1.

Table 1. Sputtering conditions.

Target composition	Bi_2O_3+In_2O_3+$PbTiO_3$+PbO, La_2O_3
Substrate	SRO (101)/Pt (200)/MgO (200)
Sputtering gas	Ar:O_2=20:1
Growth temperature	600–700℃
Sputtering pressure	0.5–2 Pa
Sputtering power	64 W
Growth rate	3–4 nm/min
Film thickness	1–3 μm
Heat treatment	Quenching at 100℃/min

The structures, morphologies, and thicknesses of xBI-$(1-x)$PT epitaxial films are measured by x-ray diffraction (XRD), scanning electron microscopy (SEM) with high resolution and surface profiler, respectively. The compositions of films are analyzed by energy dispersive spectroscopy attached to the SEM. Then, the curves of the polarization versus electric field (P–E) are obtained by the ferroelectric tester (Radiant, Premier Ⅱ), by which we evaluate the ferroelectric properties of each epitaxial film. The relative dielectric constant, dielectric loss and Curie temperature are measured using LCR meter and auxiliary heating equipment.

The ferroelectric properties of the xBI-$(1-x)$PT thin films are sensitive to the sputtering parameters including the target compositions, sputtering substrate temperatures, and gas pressures. Firstly, for the target compositions, the density functional theory calculations suggested that the MPB of xBI-$(1-x)$PT would be at $x=0.33$,[19] but in experiments, x always appeared somewhere between 0.05 and 0.20.

To explore optimum sputtering conditions for depositing xBI-$(1-x)$PT thin films with high ferroelectricity, we have adjusted the target compositions, sputtering substrate temperatures and gas pressures.

To explore the optimized xBI-$(1-x)$PT thin films deposited on SRO/Pt/MgO substrates using different BIO-PT targets under different sputtering conditions, the composition analyses of the thin films in the experiments are measured by energy dispersive spectroscopy (EDS). Table 2 lists the sputtering parameters and composition analyses of the thin films in the experiments.

Table 2. Target, sample, sputtering condition and composition of samples.

		Sputtering condition		Sample	Sample composition								
Target	Sample	Temperature (℃)	Pressure (Pa)	thickness (μm)	O (%)	Ti (%)	In (%)	Pb (%)	Bi (%)	La (%)	Pb/Ti ratio	Bi/In ratio	In/(In+Ti) ratio
A[a]	A_1	660	0.5	1.24	67.58	12.68	8.19	3.16	8.41		0.249	1.079	0.392
	A_2	670	0.5	1.20	68.78	12.42	8.12	2.35	8.33		0.189	1.026	0.395
B[b]	B_1	660	0.5	1.49	65.22	13.53	5.25	9.90	6.10		0.732	1.162	0.280
	B_2	675	0.5	1.49	67.61	12.90	5.10	6.75	7.63		0.523	1.496	0.283
	B_3	685	0.5	0.97	69.45	11.22	4.68	3.10	11.55		0.276	2.468	0.294
	B_4	700	0.5	1.10	68.13	13.67	4.74	4.52	8.94		0.331	1.886	0.258
C[c]	C_1	600	0.5	1.10	69.19	11.23	4.50	10.73	4.35		0.956	0.967	0.286
	C_2	625	0.5	1.40	66.54	13.40	4.96	10.17	4.93		0.759	0.994	0.270
	C_3	650	0.5	1.65	64.92	14.10	5.38	9.45	6.15		0.670	1.143	0.276
D[d]	D_1	650	0.5	1.00	67.19	13.80	4.58	9.92	4.06	0.46	0.719	0.887	0.249
	D_2	650	2.0	2.10	70.22	12.33	3.86	9.87	3.23	0.49	0.801	0.837	0.238

[a]A: 0.30(BIO+30%Bi_2O_3)-0.70(PT+30%PbO); [b]B: 0.20(BIO+30%Bi_2O_3)-0.80(PT+40%PbO);
[c]C: 0.20(BIO+10%Bi_2O_3)-0.80(PT+40%PbO); [d]D: 0.20(BIO+10%Bi_2O_3)-0.80(PT+40%PbO), doped 2 mol% La_2O_3.

From Table 2 it can be seen that the compositions of the thin films are different from that of the targets because of different evaporation losses of different elements and the losses are different under different deposition conditions. Therefore, to obtain excellent ferroelectric films, a series of experiments with different deposition parameters must be carried out.

Using target D, the thin films are deposited on the substrate at temperatures 650℃, and the sputtering pressures at 0.5 Pa and 2 Pa. The P–E curves of xBI-$(1-x)$PT thin films are measured at the frequency of 100 Hz, as shown in Figs. 1(D_1) and (D_2). The P–E curves exhibit typical ferroelectric behavior. However, as the sputtering pressure increases from 0.5 Pa to 2 Pa, P_r slightly increases. Figure 1(D_2) shows that the film has the optimized P–E curve, in which $2P_r$ and $2E_c$ with the applied electric field about 750 kV/cm are 80 μC/cm^2 and 300 kV/cm, re-

spectively. Under this condition, it is found that the ratios of Pb/Ti and Bi/In are 80.15% and 83.68%, respectively, which are close to the stoichiometric proportion. Meanwhile, for sample D_2, the proportion of $BiInO_3$ component is accounted as 23.8%, which indicates that the composition of the film is about 0.24BI-0.76PT, higher than 0.20BI-0.80PT of the target D_2, and close to MPB of ferroelectric materials xBI-$(1-x)$PT. Thus, the sputtering conditions for depositing the xBI-$(1-x)$PT thin films with high ferroelectricity approach to optimum.

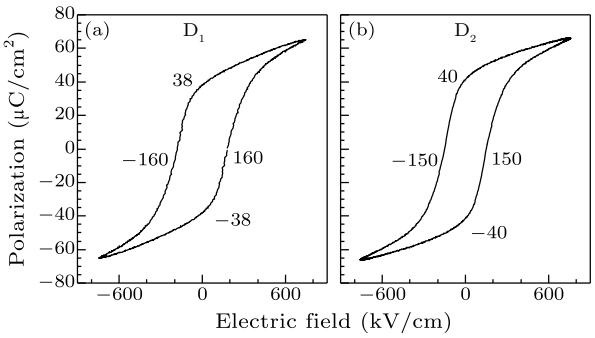

Fig. 1. The P–E curves of thin films under the optimum sputtering conditions.

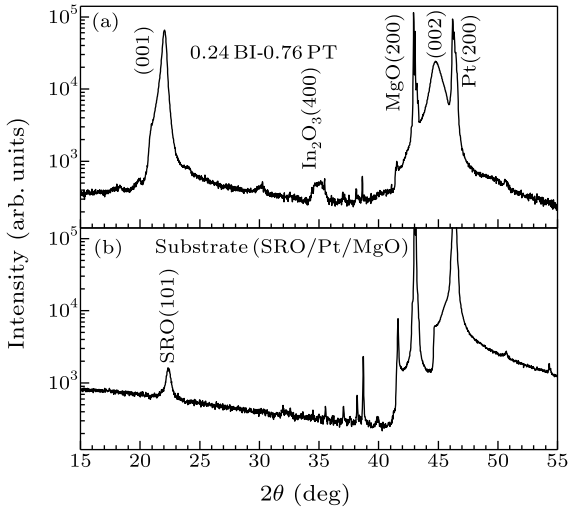

Fig. 2. Typical XRD pattern of xBI-$(1-x)$PT ($x = 0.24$).

Based on the P–E curves of the thin films, the optimum xBI-$(1-x)$PT thin films with the high ferroelectricity are deposited using the target composed of 0.20BI-0.80PT with 40% PbO-rich, 10% Bi_2O_3-rich and doped 2% La_2O_3 under sputtering pressure 2 Pa and temperature 650℃. Finally, the stoichiometric proportion of the films with the composition is about 0.24BI-0.76PT.

The crystallographic structure, morphology, ferroelectricity and Curie temperature of the excellent 0.24BI-0.76PT films are measured and described in the following.

The x-ray diffraction (XRD) patterns of the SRO/Pt/MgO substrates with and without deposited xBI-$(1-x)$PT ($x = 0.24$) thin films are shown in Fig. 2, in which strong and sharp peaks of BI-PT (001) and (002) directions are observed. It also shows a slight peak of In_2O_3 (400) near 35°. This phenomenon may indicate that the content of BI in the BI-PT films gradually reaches and exceeds the solid solubility limit of BI-PT solid solution. Therefore, the sputtered BIO-PT film is epitaxially grown on the SRO/Pt/MgO substrate, and it shows mainly (001) orientation.

The surface morphology and the cross-sectional structures of the films are measured by SEM, as shown in Figs. 3(a) and (b), respectively. The images show that the film displays multi-crystallographic structure with columnar grains arranged regularly and perpendicularly on the surface of the substrate. Meanwhile, in the cross-sectional microstructure, like the grains' shape, some In_2O_3 crystallizes; as can be observed in Fig. 2.

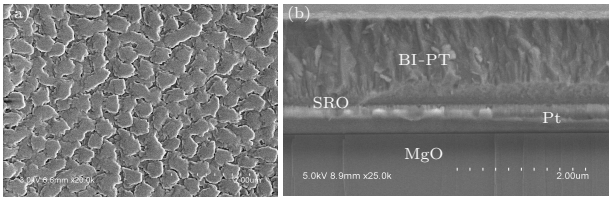

Fig. 3. (a) Scanning electron microscopy surface and (b) cross-sectional image of xBI-$(1-x)$PT ($x = 0.24$).

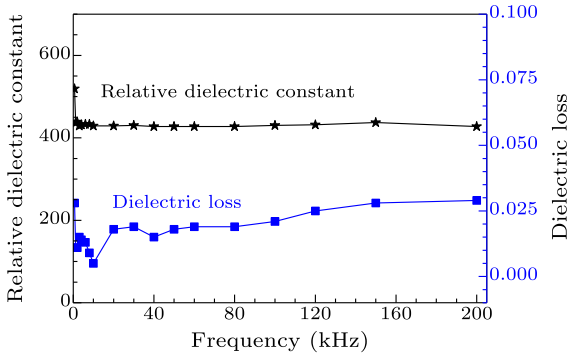

Fig. 4. The variations of ε_r and $\tan\delta$ with frequency.

The relative dielectric constant (ε_r) and dielectric loss ($\tan\delta$) of the xBI-$(1-x)$PT ($x = 0.24$) thin film with frequency relationship is measured by the LCR circuit, as shown in Fig. 4, by which ε_r and $\tan\delta$ are about 430 and 0.5%, respectively. The dispersion is not observed from 1 kHz to 200 kHz.

Using the LCR circuit combined with the heating system, ε_r and $\tan\delta$ changing with a temperature rise from 30℃ to 700℃ are obtained, as shown in Fig. 5. It is observed that ε_r and $\tan\delta$ increase slowly with increasing temperature from 30℃ to 350℃, then increase fast as a temperature higher than 350℃, till to 640℃, and then decrease obviously when the temperature is higher than 640℃.

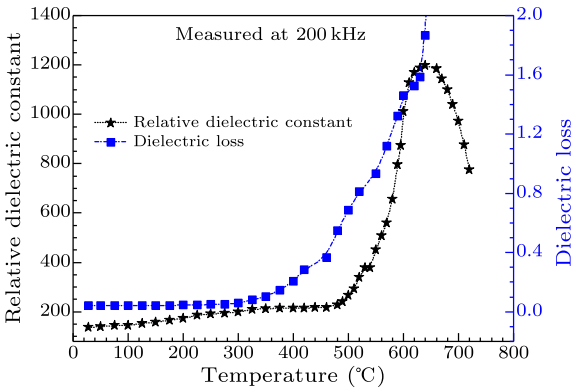

Fig. 5. The variations of ε_r and $\tan\delta$ with temperatures.

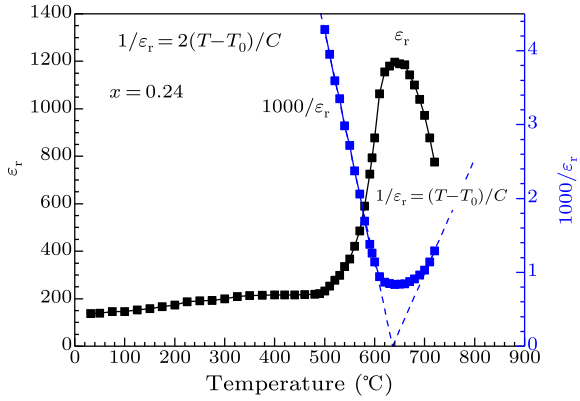

Fig. 6. The variations of ε_r and $\tan\delta$ with temperatures.

Meanwhile, the dielectric loss is larger than 1, when the temperature is more significant than 500℃. The dielectric loss with more than 1 indicates that the specimen may be a resister rather than a capacitor, which indicates that T_c is more significant than 500℃.

To further study the ferroelectric phase transition at the Curie temperature, the Curie–Weiss law is used to check the transitions of the xBI-$(1-x)$PT thin films, which is expressed as[20]

$$1/\varepsilon_r \propto (T - T_0)/C, \tag{1}$$

where T_0 is the Curie–Weiss temperature, and C is the Curie constant. In general, the dielectric constants versus temperature in the ferroelectric phase ($T \leqslant T_0$) and paraelectric phase ($T > T_0$) can be expressed as

$$1/\varepsilon_r = -2(T - T_0)/C,\ T \leqslant T_0, \tag{2}$$

$$1/\varepsilon_r = (T - T_0)/C,\ T > T_0. \tag{3}$$

Based on Fig. 5, the reciprocal dielectric constants $(1/\varepsilon_r)$ versus temperature (T) of the film can be obtained by Eqs. (2) and (3), which are shown in Fig. 6. The Curie–Weiss temperature (T_0) is approximately 636℃, which almost agrees with the Curie temperature T_c, where the Curie constant $C = 6.88 \times 10^4$℃ $(T > T_0)$ and $C = 6.32 \times 10^4$℃ $(T > T_0)$. The results indicate that the sputtered thin films obey the Curie–Weiss law and undergo complete ferroelectric transition around the Curie point and belong to the second-order phase transition.

In summary, the chemical compositions of the sputtered xBI-$(1-x)$PT thin films are different from that of the targets because the former is dependent on the sputtering conditions, such as the evaporations of some elements at different temperatures and pressures. By adjusting the sputtering parameters, the xBI-$(1-x)$PT thin films deposited on (200) MgO crystal substrates using the rf-magnetron sputtering method are optimized. The optimized thin film xBI-$(1-x)$PT ($x = 0.24$) exhibits extraordinary ferroelectricity, such as large $2P_r = 80\,\mu C/cm^2$ and $2E_c = 300\,kV/cm$, respectively. The Curie temperatures (T_c) with 640℃ of the xBI-$(1-x)$PT thin films are obtained. The sputtered thin films obey the Curie–Weiss law, and undergo complete ferroelectric transition around the Curie point and belong to the second-order phase transition.

Overall, the optimized thin films described in this Letter have high ferroelectricity and high T_c. Therefore, they are promising thin film materials for high-temperature ferroelectric applications. Meanwhile, this work illustrates that the optimized compositions and structures can control the properties of the films. The favorite films have wide potential to be applied in new electric devices that are operated in harsh conditions for applications in automobile, aerospace industries and related industrial applications.

References

[1] Zhang T et al 2008 *J. Vac. Sci. Technol.* **26** 985
[2] Zhu B P et al 2009 *Appl. Phys. Lett.* **94** 102901
[3] Bronson J R et al 2009 *Proc. IEEE Micro Electro Mech. Syst.* 1047
[4] Zhang T et al 2009 *Appl. Phys. Lett.* **94** 122909
[5] Datta K et al 2009 *Appl. Phys. Lett.* **95** 251901
[6] Eitel R E et al 2001 *Jpn. J. Appl. Phys.* **40** 5999
[7] Duan R et al 2004 *J. Mater. Res.* **19** 2185
[8] Sun K X et al 2018 *Jpn. J. Appl. Phys.* **57** 025801
[9] Ko S W et al 2009 *Appl. Phys. Lett.* **95** 162901
[10] Zhang L X et al 2014 *Ceram. Int.* **40** 6307
[11] Lee S Y et al 2012 *Appl. Phys. Lett.* **100** 212905
[12] Lee S Y et al 2014 *J. Appl. Phys.* **115** 224105
[13] Wasa K et al 2012 *IEEE Trans. Ultrason. Ferroelectr. Freq. Control* **59** 6
[14] Wang Y et al 2015 *Chin. Phys. Lett.* **32** 086802
[15] Sun K X et al 2016 *Phys. Status Solidi* A **213** 2479
[16] Zhong X L et al 2004 *Appl. Phys. Lett.* **85** 5661
[17] Wasa K, Adachi H and Kitabatake M 2004 *Thin Film Materials Technology: Sputtering of Compound Materials* (New York: Springer) p 171
[18] Sun K X, Zhang S Y, Wasa K and Shui X J 2016 *Chin. Phys. Lett.* **33** 064301
[19] Grinberg I, Suchomel M, Davies P and Rappe A 2005 *J. Appl. Phys.* **98** 094111
[20] Wasa K, Matsushima T, Adachi H, Matsunaga T, Yanagitani T and Yamamoto T 2015 *J. Appl. Phys.* **117** 124106